Electronic Supplementary Information

Experimental section

Materials: GO, commercial TiO_2 powder, ammonium chloride (NH_4Cl), hydrazine hydrate ($N_2H_4 \cdot H_2O$), sodium hypochlorite (NaClO), sodium hydroxide (NaOH), sodium salicylate ($C_7H_5O_3Na$), sodium sulfate (Na_2SO_4), hydrochloric acid (HCl), ethanol (CH_3CH_2OH), and carbon paper were bought from Beijing Chemical Corporation. Para-(dimethylamino) benzaldehyde ($C_9H_{11}NO$), sodium nitroferricyanide (III) dihydrate ($Na_2Fe(CN)_5NO \cdot 2H_2O$), and Nafion were purchased from Aladdin Ltd. (Shanghai, China). The water used throughout all experiments was purified through a Millipore system.

Preparation of TiO_2-rGO: TiO_2 powder was dissolved in homogeneous GO aqueous dispersion under stirring for about 1 h. After that, the mixture was sealed in a 50 mL Teflon-lined autoclave and maintained at 180 °C for 2 h. The autoclave was naturally cooled down to room temperature. Finally, a black cylinder was obtained.

Preparation of TiO_2-rGO/CP electrode: 10 mg TiO_2-rGO powders and 20 μL of Nafion solution (5 wt%) were dispersed in 980 μL mixed solution contain 600 μL ethanol and 380 μL H_2O by 2 h sonication to form a homogeneous ink. Then, 10 μL TiO_2-rGO was loaded on a CP with area of 0.5 x 0.5 cm^2 and dried under ambient condition.

Characterizations: XRD patterns were obtained from a Shimazu XRD-6100 diffractometer with Cu Kα radiation (40 kV, 30 mA) of wavelength 0.154 nm (Japan). SEM images were collected from the tungsten lamp-equipped SU3500 scanning electron microscope at an accelerating voltage of 20 kV (HITACHI, Japan). Scanning electron microscope (SEM) measurements were recorded on a XL30 ESEM FEG scanning electron microscope at an accelerating voltage of 20 kV. TEM images were obtained from a Zeiss Libra 200FE transmission electron microscope operated at 200 kV. XPS measurements were performed on an ESCALABMK II X-ray photoelectron spectrometer using Mg as the exciting source. The absorbance data of spectrophotometer were measured on SHIMADZU UV-1800 ultraviolet-visible (UV-

Vis) spectrophotometer. Thermogravimetric analysis (TGA) was performed on a Perkin-Elmer Model Pyris1 TGA apparatus at a heating rate of 10 °C min^{-1} in nitrogen atmosphere.

Electrochemical measurements: Electrochemical measurements were performed with a CHI 660E electrochemical analyzer (CH Instruments, Inc., Shanghai) using a standard three-electrode system using TiO_2-rGO/CP as the working electrode, graphite rod as the counter electrode, and saturated Ag/AgCl electrode as the reference electrode. In all measurements, saturated Ag/AgCl electrode was calibrated with respect to reversible hydrogen electrode as following: in 0.1 M Na_2SO_4 aqueous solution, $E(RHE) = E(Ag/AgCl) + 0.059 \times pH + 0.197$ V. All experiments were carried out at room temperature. For N_2 reduction experiments, the 0.1 M Na_2SO_4 electrolyte was purged with N_2 for 30 min before the measurement. Potentiostatic test was conducted in N_2-saturated 0.1 M Na_2SO_4 solution (35 mL) in a two-compartment cell, which was separated by Nafion 211 membrane.

Determination of NH_3: The concentration of NH_4^+ was prepared as follows. Firstly, 50 μg mL^{-1} NH_4^+ solution was prepared and diluted to 1 μg mL^{-1}. Then, 0.0, 0.5, 1.0, 1.5, 2.0, 2.5, 3.0 mL NH_4^+ solution with concentration of 1 μg mL^{-1} were poured into 10 mL test tubes and separately diluted to 10 mL with 0.1 M Na_2SO_4 and the resulting concentrations of NH_4^+ in the solutions are 0.00, 0.05, 0.10, 0.15, 0.20, 0.25, 0.30 μg mL^{-1}. The produced NH_3 was detected with indophenol blue by ultraviolet spectroscopy.[1] In detail, 4 mL electrolyte was obatined from the cathodic chamber and mixed with 50 μL oxidizing solution containing NaClO ($\rho Cl = 4 \sim 4.9$) and NaOH (0.75 M), 500 μL coloring solution containing 0.4 M $C_7H_6O_3$ and 0.32 M NaOH, and 50 μL catalyst solution (1 wt% $Na_2[Fe(CN)_5NO]$) for 2 h. Absorbance measurements were performed at $\lambda = 660$ nm. The concentration-absorbance curve was calibrated using standard NH_4^+ solution with a serious of concentrations. The fitting curve ($y = 0.682x + 0.029$, $R^2 = 0.999$) shows good linear relation of absorbance value with NH_4^+ concentration.

Determination of N_2H_4: The concentration of N_2H_4 was prepared as follows. Firstly, 2 mg mL^{-1} N_2H_4 solution was prepared and diluted to 2 μg mL^{-1}. Then, 0.0, 0.5, 1.0, 1.5, 2.0, 2.5, 5.0 mL N_2H_4 solution with concentration of 2 μg mL^{-1} were poured into 10 mL test tubes and separately diluted to 5 mL with 0.1 M Na_2SO_4 and the resulting concentrations of N_2H_4 in the solutions are 0.0, 0.2, 0.4, 0.6, 0.8, 1.0, 2.0 μg mL^{-1}. The N_2H_4 present in the electrolyte was determined by the method of Watt and Chrisp.[2] The mixture of $C_9H_{11}NO$ (5.99 g), HCl (30 mL), and C_2H_5OH (300 mL) was used as a color reagent. In detail, 5 mL electrolyte was removed from the electrochemical reaction vessel, and added into 5 mL above prepared color reagent and stirring 10 min at room temperature. Moreover, the absorbance of the resulting solution was measured at a wavelength of 455 nm. The concentration absorbance curves were calibrated using standard N_2H_4 solution with a series of concentrations. The fitting curve ($y = 0.4909x + 0.047$, $R^2 = 0.999$) shows good linear relation of absorbance value with N_2H_4 concentration.

Calculations of NH_3 formation rate and FE: NH_3 formation rate was calculated using the following equation:

$$NH_3 \text{ formation rate} = [NH_4^+] \times V/(m_{cat.} \times t)$$

FE was calculated according to following equation:

$$FE = 3 \times F \times [NH_4^+] \times V/(18 \times Q)$$

Where $[NH_4^+]$ is the measured NH_4^+ concentration; V is the volume of the cathodic reaction electrolyte; t is the potential applied time; $m_{cat.}$ is the loaded quality of catalyst; F is the Faraday constant; and Q is the quantity of applied electricity

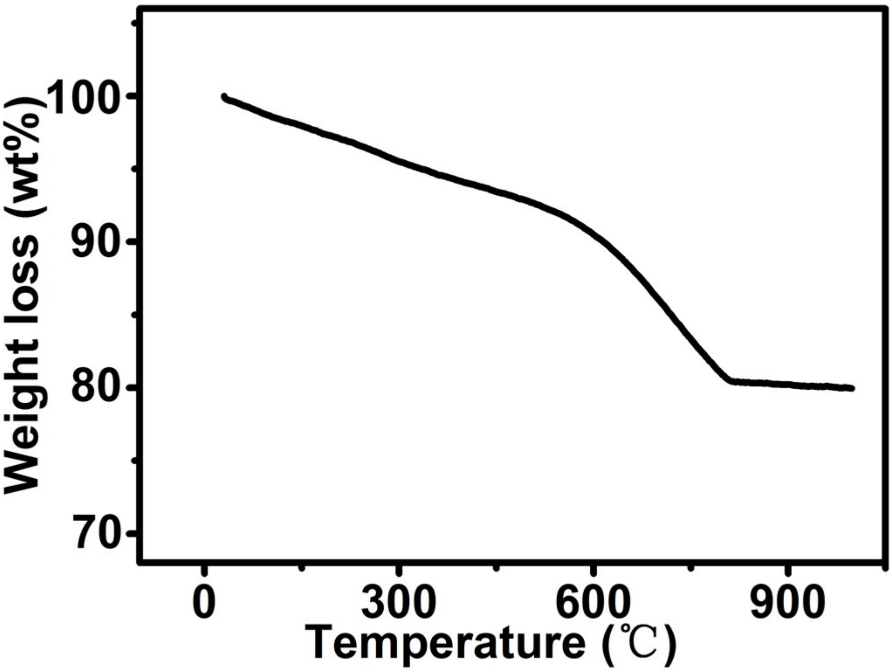

Fig. S1. TGA curve of TiO_2-rGO.

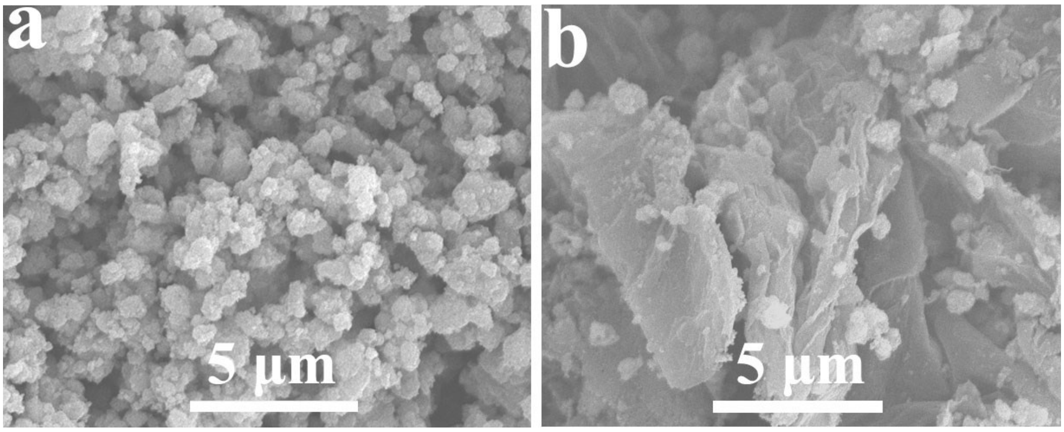

Fig. S2. SEM images of TiO_2 and TiO_2-rGO.

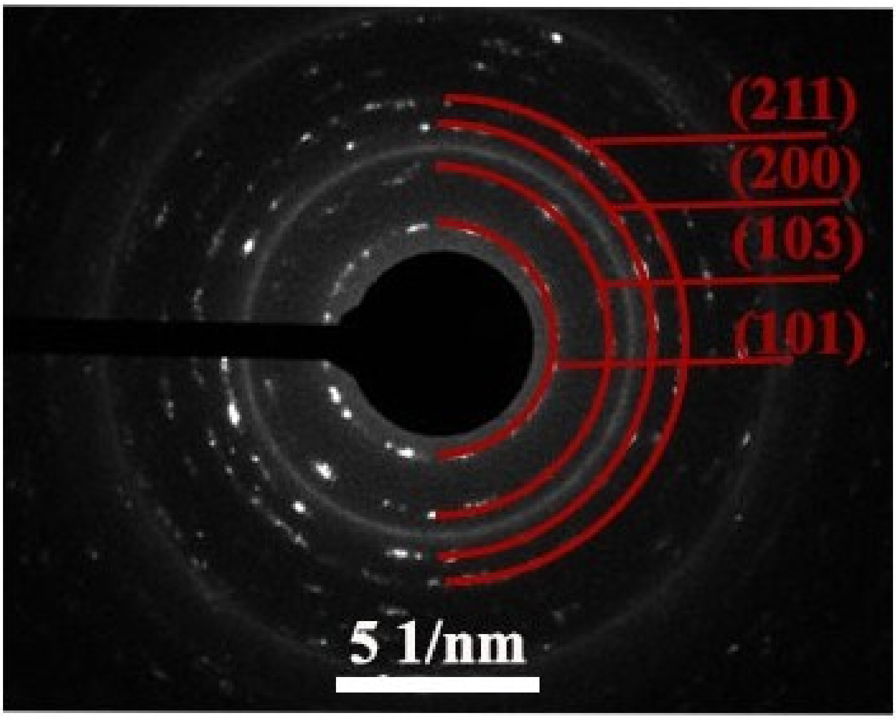

Fig. S3. SAED pattern taken from TiO_2-rGO.

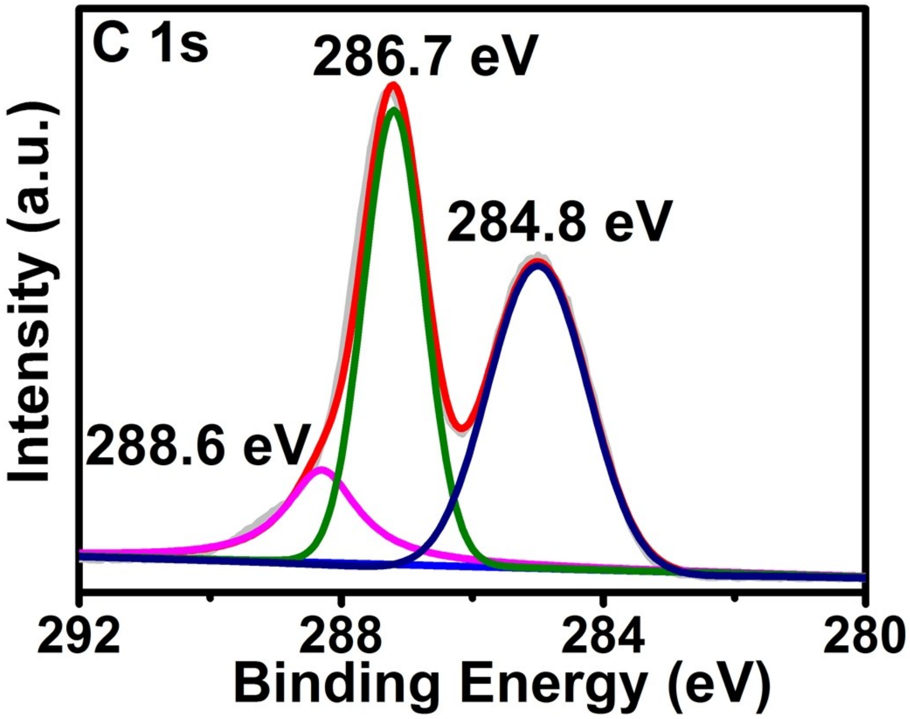

Fig. S4. XPS spectrum of GO in the C 1s.

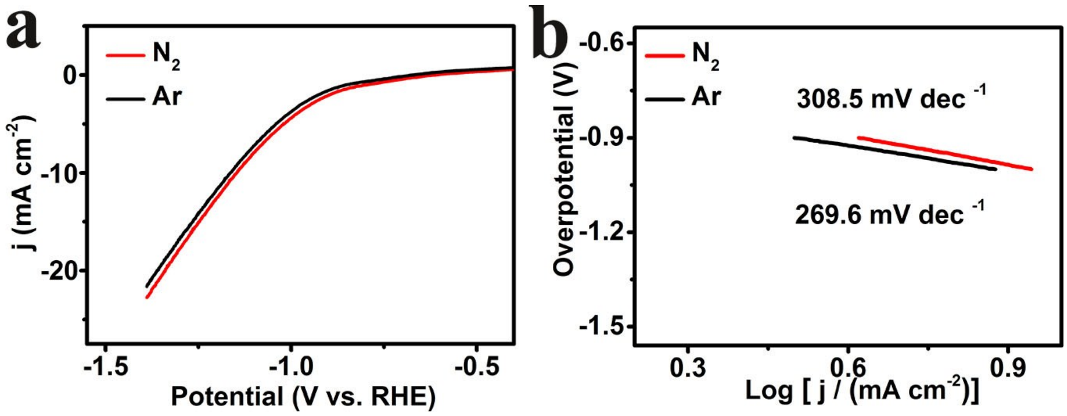

Fig. S5. (a) LSV curves and (b) corresponding Tafel plots of TiO_2-rGO/CP in Ar- and N_2-saturated 0.1 M Na_2SO_4.

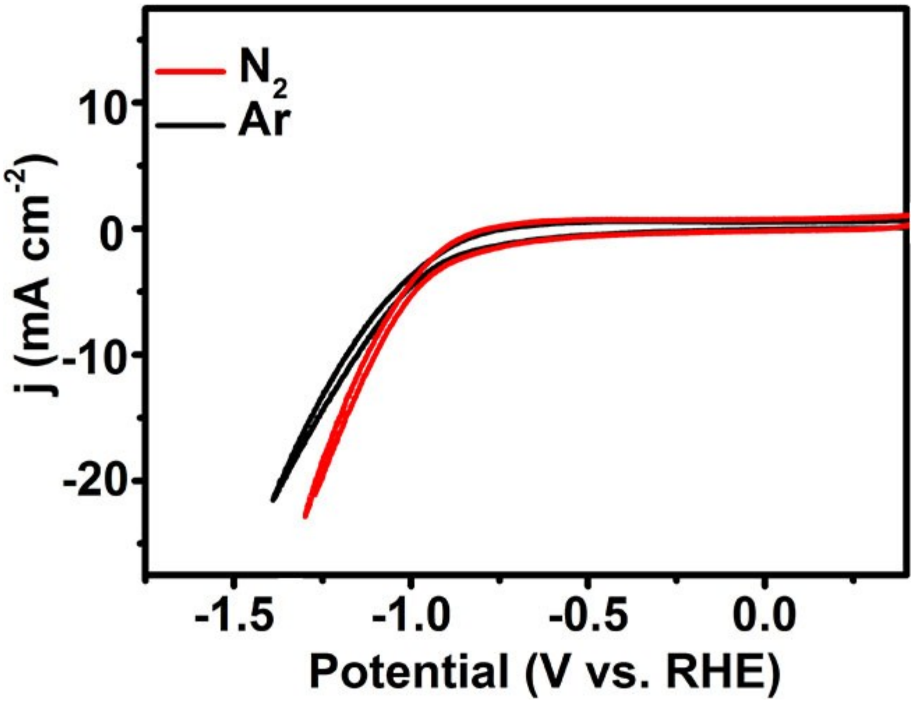

Fig. S6. CV curves of TiO_2-rGO/CP in Ar- and N_2-saturated 0.1 M Na_2SO_4.

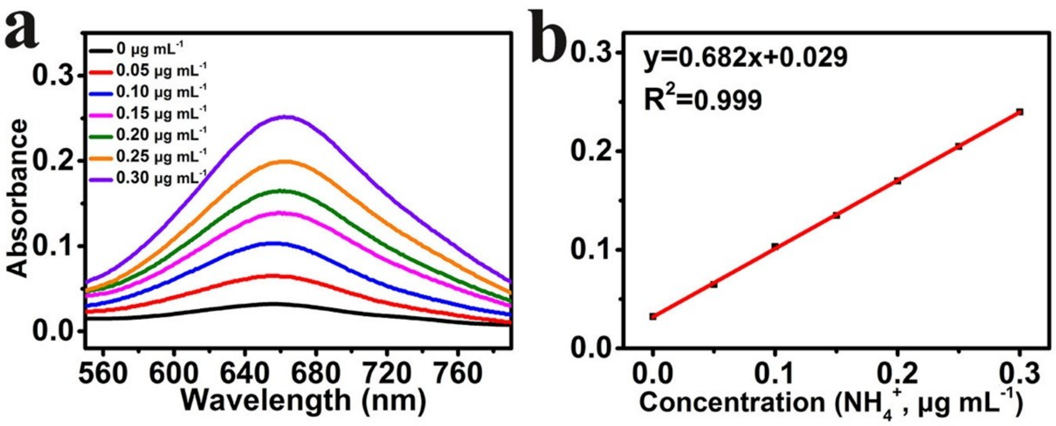

Fig. S7. (a) UV-Vis absorption spectra of indophenol assays with NH_4^+ concentrations after incubated for 2 h at room temperature. (b) Calibration curve used for calculation of NH_4^+ concentrations.

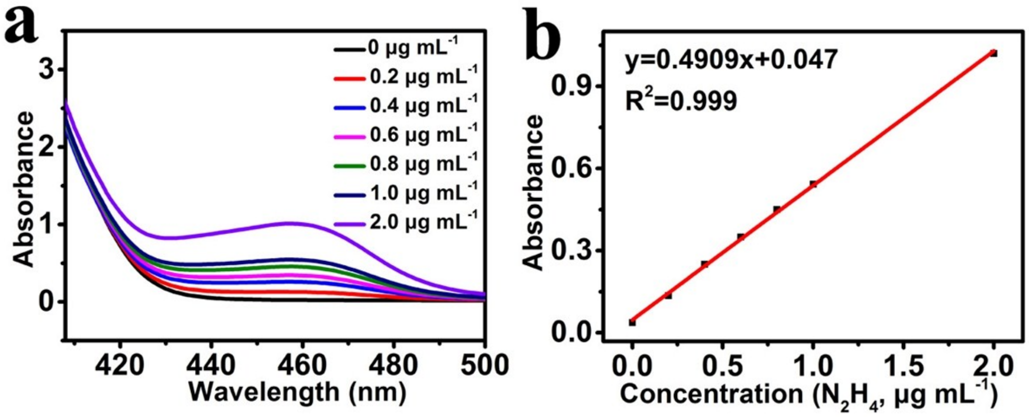

Fig. S8. (a) UV-Vis absorption spectra of various N_2H_4 concentrations after incubated for 10 min at room temperature. (b) Calibration curve used for calculation of N_2H_4 concentrations.

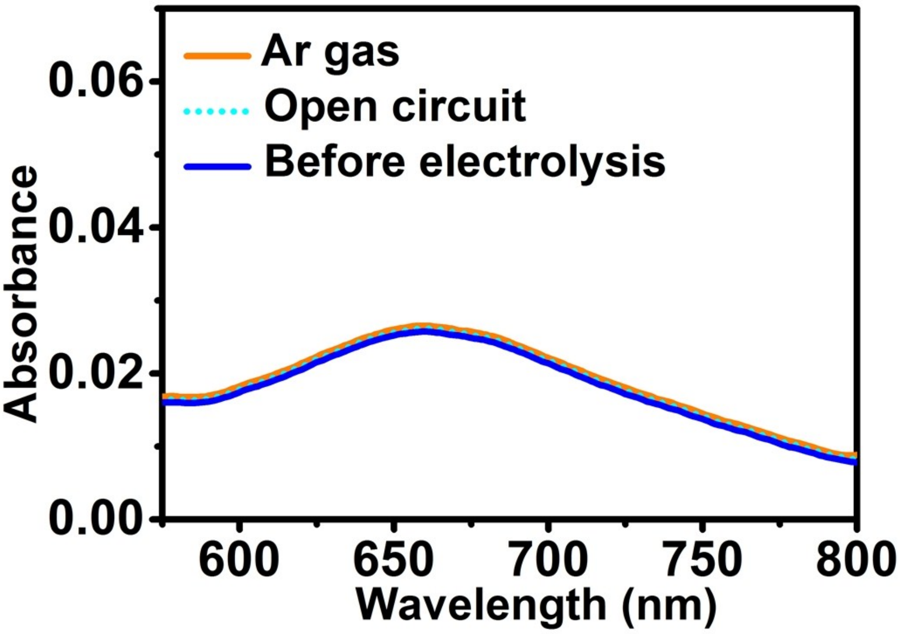

Fig. S9. UV-Vis absorption spectra of electrolytes stained with indophenol indicator before and after 2 h electrolysis at the potential of –0.90 V under different electrochemical conditions.

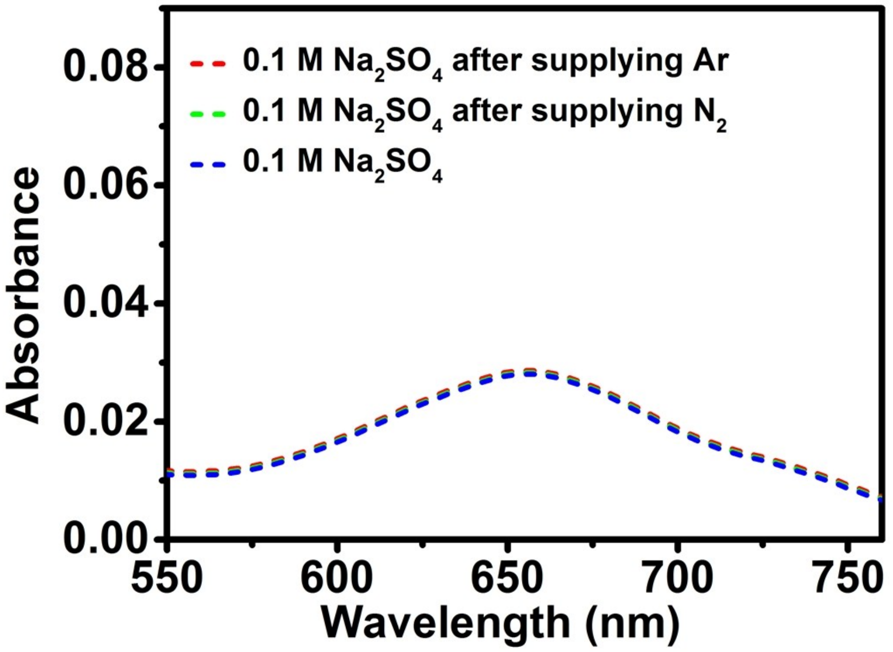

Fig. S10. UV-Vis absorption spectra of the 0.1 M Na_2SO_4 electrolyte stained with indophenol indicator after continuously supplying N_2 or Ar with no applied voltage.

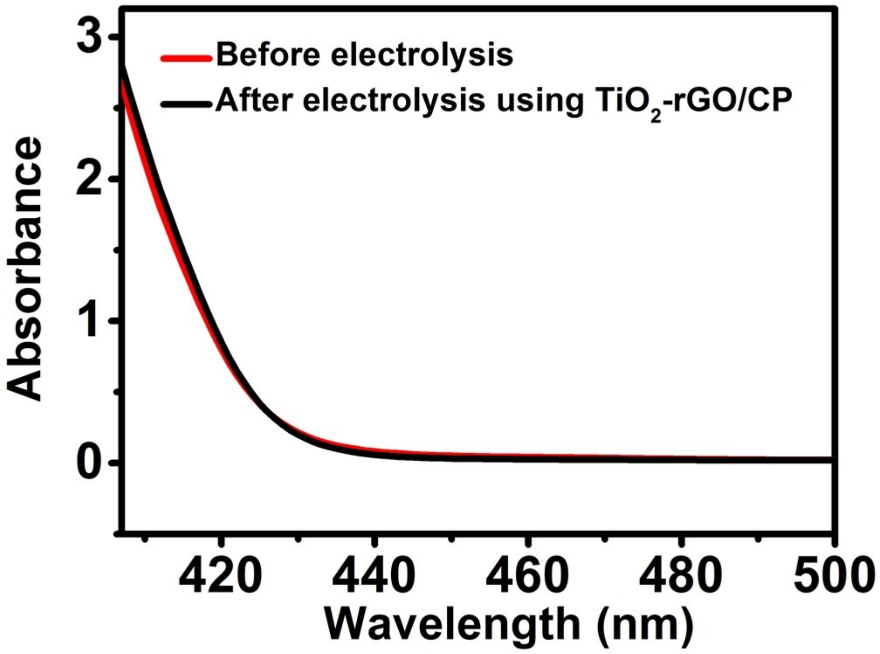

Fig. S11. UV-Vis absorption spectra of the electrolytes estimated by the method of Watt and Chrisp before and after 2 h electrolysis in N_2 atmosphere at –0.90 V.

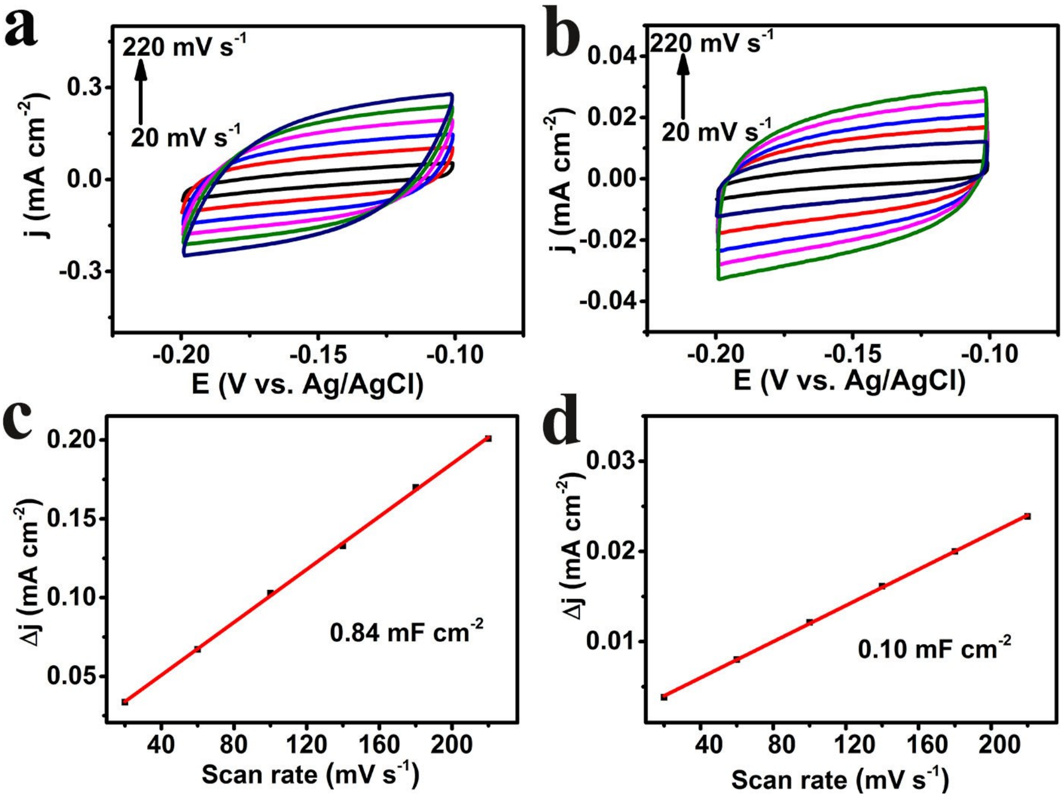

Fig. S12. CVs of (a) TiO_2-rGO/CP and (b) TiO_2/CP with various scan rates (20-220 mV s^{-1}) in the region of –0.1 to –0.2 V vs. Ag/AgCl. The capacitive current densities at –0.15 V vs. Ag/AgCl as a function of scan rates for (c) TiO_2-rGO/CP and (d) TiO_2/CP.

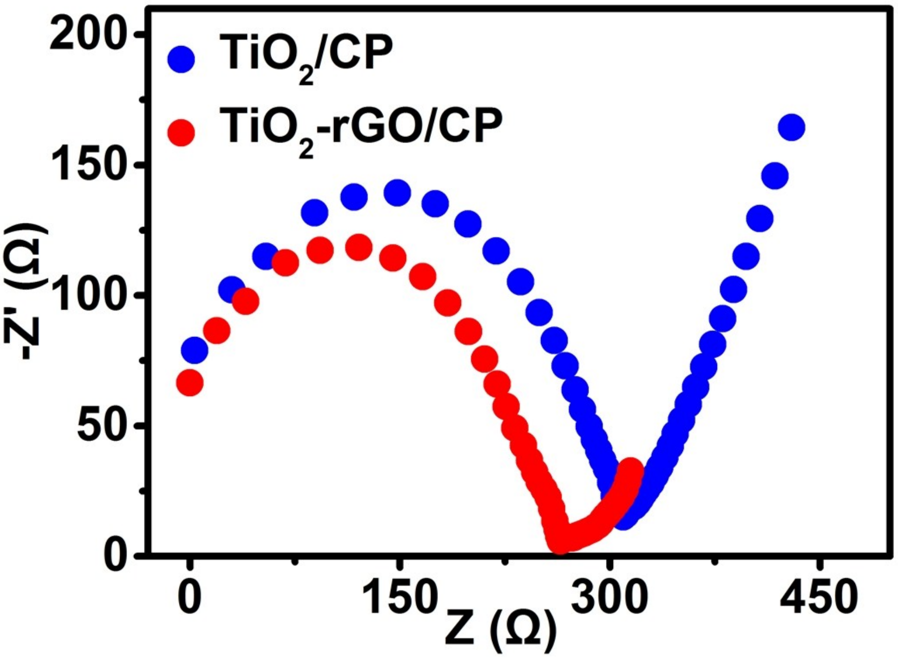

Fig. S13. Nyquist plots of TiO_2-rGO/CP and TiO_2-/CP.

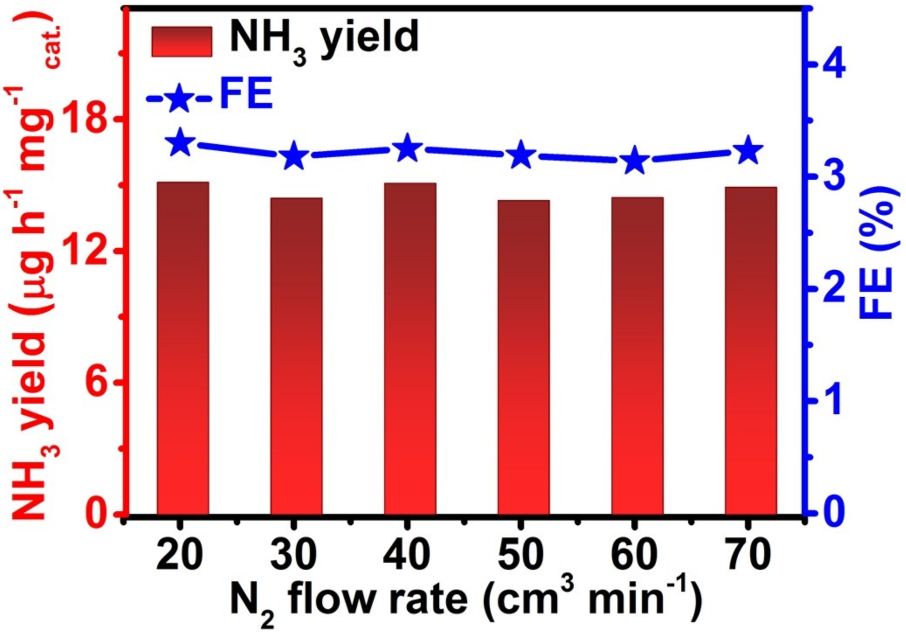

Fig. S14. NH_3 yields and FEs of TiO_2-rGO/CP with different N_2 flow rate.

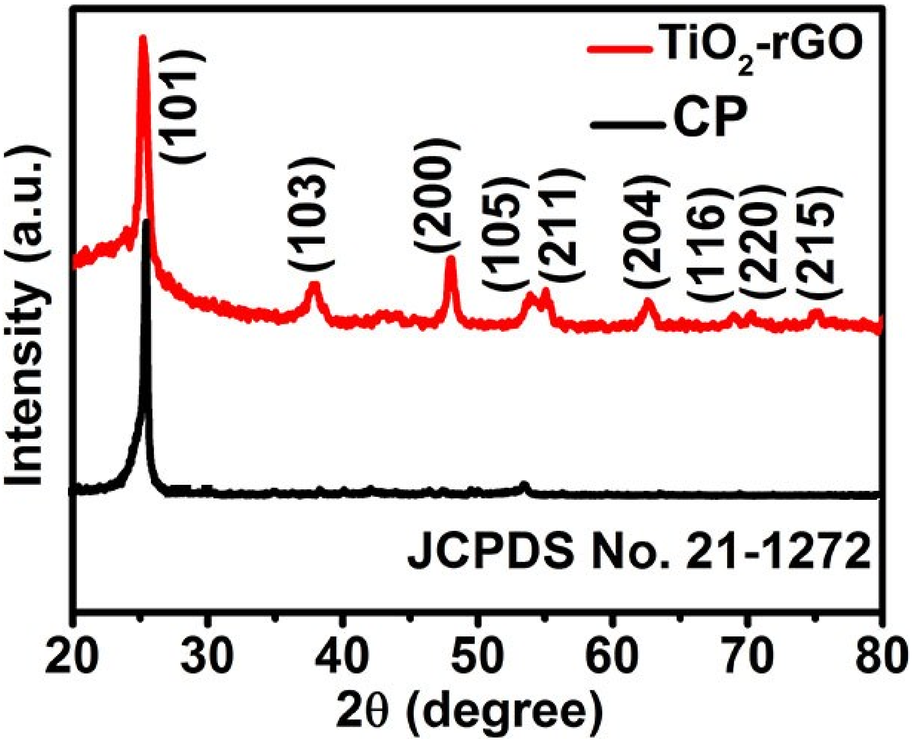

Fig. S15. XRD patterns for CP and TiO_2-rGO/CP after long-term electrolytic reaction in 0.1 M Na_2SO_4.

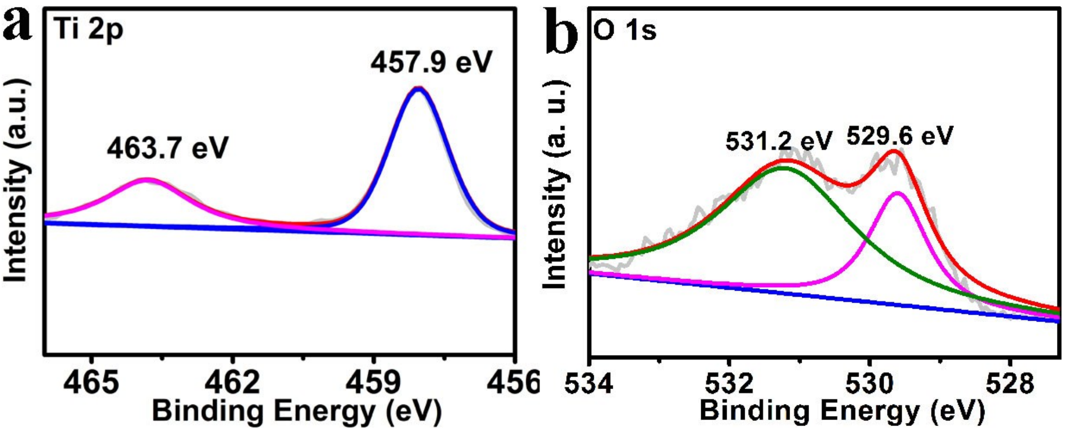

Fig. S16. XPS spectra in the (a) Ti 2p and (b) O 1s regions after long-term electrolytic reaction in 0.1 M Na_2SO_4.

Table S1. Comparison of the electrocatalytic NRR performance of TiO_2-rGO with other aqueous-based NRR electrocatalysts at room temperature.

Catalyst	**Electrolyte**	**NH_3 yield**	**FE (%)**	**Ref.**
TiO_2-rGO	0.1 M Na_2SO_4	15.13 μg h^{-1} $mg^{-1}_{cat.}$	3.3	This work
Au nanorods	0.1 M KOH	6.042 μg h^{-1} $mg^{-1}_{cat.}$	4	3
α-Au/CeO_x-RGO	0.1 M HCl	8.31 μg h^{-1} $mg^{-1}_{cat.}$	10.1	4
TA-reduced Au/TiO_2	0.1 M HCl	21.4 μg h^{-1} $mg^{-1}_{cat.}$	8.11	5
Pd/C	0.1 M PBS	4.5 μg h^{-1} $mg^{-1}_{cat.}$	8.2	6
Ru/C	2.0 M KOH	0.21 μg h^{-1} cm^{-2}	0.28	7
NPC	0.05 M H_2SO_4	23.8 μg h^{-1} $mg^{-1}_{cat.}$	1.42	8
γ-Fe_2O_3	0.1 M KOH	0.212 μg h^{-1} $mg^{-1}_{cat.}$	1.9	9
$Bi_4V_2O_{11}$/CeO_2	0.1 M HCl	23.21 μg h^{-1} $mg^{-1}_{cat.}$	10.16	10
MoS_2/CC	0.1 M Na_2SO_4	4.94 μg h^{-1} cm^{-2}	1.17	11
Mo_2N	0.1 M HCl	78.4 μg h^{-1} $mg^{-1}_{cat.}$	4.5	12
MoN NA/CC	0.1 M HCl	3.01×10^{-10} mol s^{-1} cm^{-2}	1.15	13
Mo nanofilm	0.01 M H_2SO_4	1.89 μg h^{-1} cm^{-2}	0.72	14
PEBCD/C	0.5 M Li_2SO_4	1.58 μg h^{-1} cm^{-2}	2.85	15
Fe_2O_3-CNT	$KHCO_3$	0.22 μg h^{-1} cm^{-2}	0.15	16
Fe_3O_4/Ti	0.1 M Na_2SO_4	3.43 μg h^{-1} cm^{-2}	2.6	17
MoO_3	0.1 M HCl	29.43 μg h^{-1} $mg^{-1}_{cat.}$	1.9	18
VN/TM	0.1 M HCl	5.14 μg h^{-1} cm^{-2}	2.25	19
Nb_2O_5 nanofiber	0.1 M HCl	43.6 μg h^{-1} $mg^{-1}_{cat.}$	9.26	20

References

1 D. Zhu, L. Zhang, R. E. Ruther and R. J. Hamers, *Nat. Mater.*, 2013, **12**, 836–841.

2 G. W. Watt and J. D. Chrisp, *Anal. Chem.*, 1952, **24**, 2006–2008.

3 D. Bao, Q. Zhang, F. Meng, H. Zhong, M. Shi, Y. Zhang, J. Yan, Q. Jiang and X. Zhang, *Adv. Mater.*, 2017, **29**, 1604799.

4 S. Li, D. Bao, M. Shi, B. Wulan, J. Yan and Q. Jiang, *Adv. Mater.*, 2017, **29**, 1700001.

5 M. Shi, D. Bao, B. Wulan, Y. Li, Y. Zhang, J. Yan and Q. Jiang, *Adv. Mater.*, 2017, **29**, 1606550.

6 J. Wang, L. Yu, L. Hu, G. Chen, H. Xin and X. Feng, *Nat. Commun.*, 2018, **9**, 1795.

7 V. Kordali, G. Kyriacou and C. Lambrou, *Chem. Commun.*, 2000, **17**, 1673–1674.

8 Y. Liu, Y. Su, X. Quan, X. Fan, S. Chen, H. Yu, H. Zhao, Y. Zhang and J. Zhao, *ACS Catal.*, 2018, **8**, 1186–1191.

9 J. Kong, A. Lim, C. Yoon, J. H. Jang, H. C. Ham, J. Han, S. Nam, D. Kim, Y. E. Sung, J. Choi and H. S. Park, *ACS Sustainable Chem. Eng.*, 2017, **5**, 10986–10995.

10 C. Lv, C. Yan, G. Chen, Y. Ding, J. Sun, Y. Zhou and G. Yu, *Angew. Chem., Int. Ed.*, 2018, **57**, 6073–6076.

11 L. Zhang, X. Ji, X. Ren, Y. Ma, X. Shi, Z. Tian, A. M. Asiri, L. Chen, B. Tang and X. Sun, *Adv. Mater.*, **30**, 1800191.

12 X. Ren, G. Cui, L. Chen, F. Xie, Q. Wei, Z. Tian and X. Sun, *Chem. Commun.*, 2018, **54**, 8474–8477.

13 L. Zhang, X. Ji, X. Ren, Y. Luo, X. Shi, A. M. Asiri, B. Zheng and X. Sun, *ACS Sustainable Chem. Eng.*, 2018, DOI: 10.1021/acssuschemeng.8b01438.

14 D. Yang, T. Chen and Z. Wang, *J. Mater. Chem. A*, 2017, **5**, 18967–18971.

15 G. Chen, X. Cao, S. Wu, X. Zeng, L. Ding, M. Zhu and H. Wang, *J. Am. Chem. Soc.*, 2017, **139**, 9771–9774.

16 S. Chen, S. Perathoner, C. Ampelli, C. Mebrahtu, D. Su and G. Centi, *Angew. Chem., Int. Ed.*, 2017, **56**, 2699–2703.

17 Q. Liu, X. Zhang, B. Zhang, Y. Luo, G. Cui, F. Xie, A. M. Asiri and X. Sun, *Nanoscale*, 2018, **10**, 14386–14389.

18 J. Han, X. Ji, X. Ren, G. Cui, L. Li, F. Xie, H. Wang, B. Li and X. Sun, *J. Mater. Chem. A*, 2018, **6**, 12974–12977.

19 R. Zhang, Y. Zhang, X. Ren, G. Cui, A. M. Asiri, B. Zheng and X. Sun, *ACS Sustainable Chem. Eng.*, 2018, DOI: 10.1021/acssuschemeng.8b01261.

20 J. Han, Z. Liu, Y. Ma, G. Cui, F. Xie, F. Wang, Y. Wu, S. Gao, Y. Xu and X. Sun, *Nano Energy,* 2018, DOI: 10.1016/j.nanoen.2018.07.045.